Desalination and Water Treatment
www.deswater.com
doi: 10.5004/dwt.2021.26508

209 (2021) 1–15
January

Energy and exergy analysis of a solar/hybrid humidification–dehumidification desalination system

Wael Abdelmoez*, Noha M. Sayed, Eman A. Ashour

Department of Chemical Engineering, Faculty of Engineering, Minia University, 61516 Minia, Egypt, Tel. +20 100 0859791; Fax: +20 86 2346674; emails: drengwael2003@yahoo.com (W. Abdelmoez), noha.mohammed63@yahoo.com (N.M. Sayed), emanalyashour@yahoo.com (E.A. Ashour)

Received 12 May 2020; Accepted 22 August 2020

ABSTRACT

Conventional energy and exergy analyses were performed for solar/hybrid humidification–dehumidification and heating (HDH) desalination systems. An experimental investigation of HDH productivity under various operating conditions was also performed. The three major objectives of this work were to investigate the maximum productivity of solar and hybrid HDH systems, identify the locations where the largest exergetic destructions occur, and compare the results of conventional energy and exergy analyses. The prototype was constructed and designed in the Solar Energy Laboratory at the Faculty of Engineering, Chemical Engineering Department, Minia University, Egypt. It was composed of a flat-plate solar collector (product of Inter Solar Egypt Company, Egypt), a packed-bed humidifier, dehumidifier, and an additional gas heater. Different experiments were carried out to identify the factors that influence HDH system performance and exergy destruction, such as the temperatures and flow rates of air and saline water. The experimental results showed that the productivity of the system increased with increasing flow rates of air and saline water. The highest productivity was 3 and 8.8 kg/h for the solar and hybrid HDH systems, respectively. The exergy analysis showed that, for the solar heating system, the highest exergetic destruction occurred in the flat-plate solar collectors. In the hybrid HDH system, the largest exergetic destruction occurred in the dehumidifier, which can be decreased by increasing the inlet saline water temperature. The exergetic efficiency of the humidifier was found to be improved by decreasing the inlet saline water flow rate. In addition, exergetic destruction in the humidifier was reduced by decreasing the inlet air temperature.

Keywords: Conventional energy analysis; Exergy analysis; HDH; Exergy destruction

1. Introduction

The worldwide availability of freshwater is steadily decreasing because of climate change, industrialization, and a dramatic increase in population. In the near future, a large gap between freshwater demand and supply is expected to develop and to extend to other regions. The desalination of saline water, which is abundant in seas and oceans, is considered the most suitable solution to this future problem. Accordingly, researchers have been developing optimal, efficient, and low-cost desalination technologies. Various desalination processes, which can be categorized into thermal, mechanical, electrochemical, and membrane filtration technologies, have emerged from these efforts.

Among the thermal processes, humidification–dehumidification technology, which mimics the natural water cycle, is an emergent and promising desalination process. Humidification–dehumidification and heating (HDH) systems have been developed to operate on the same principles

* Corresponding author.

as solar stills; however, the main processes in solar stills are carried out in the same unit, resulting in low system efficiency. Consequently, in HDH, each process is separated into an individual unit, which enhances system productivity and performance [1]. Conventional desalination processes consume a large amount of fossil fuels, thereby generating a large amount of CO_2 emissions. To avoid this issue, the use of renewable energy, especially solar energy, is critical. HDH is a simple technology that can be powered by a low-grade source of energy or by solar energy. In HDH, seawater is desalinated by carrying of water vapor using air in a humidifier. Condensation then occurs in a dehumidifier because of the indirect contact between cold saline water and hot humid air, as shown in Fig. 1.

Numerous investigations of the productivity of HDH systems with various configurations and different energy sources have recently been reported [3–10]. For example, Lawal et al. [4] used the waste heat from a mechanical vapor compression refrigeration cycle (heat pump) to power a HDH desalination unit. They evaluated the influence of various parameters such as the saline water temperature, feedwater flow rate, feed mass flow rate ratio, and chilled water temperature. Their results showed that both the feedwater temperature and mass flow rate ratio significantly affected the proposed system. The maximum productivity was 287.8 L/d with a 4.07 gained output ratio (GOR) and 4.86% COP. The cost of freshwater was found to be 10.68 to 20.39 USD/m^3. Gao et al. [11] used a similar approach to investigate the performance of a HDH unit powered by a mechanical vapor compression pump. They used a packed-bed humidifier (450 mm × 450 mm × 300 mm) called an alveolate humidifier, which contained a honeycomb paper packing material with a large evaporation surface area. This unit provided two advantages: first, it used a heat-pump condenser and evaporator as a cooling and heating source, respectively, resulting in a compact system. Second, it used solar energy as a clean and low-cost heat source. A mathematical model was judiciously developed for the desalination unit based on mass and heat transfer in the packed humidifier. The authors investigated the effect of numerous parameters, including the air and water mass flow rates and temperatures. The freshwater production rate increased with increasing solar insolation and vice versa.

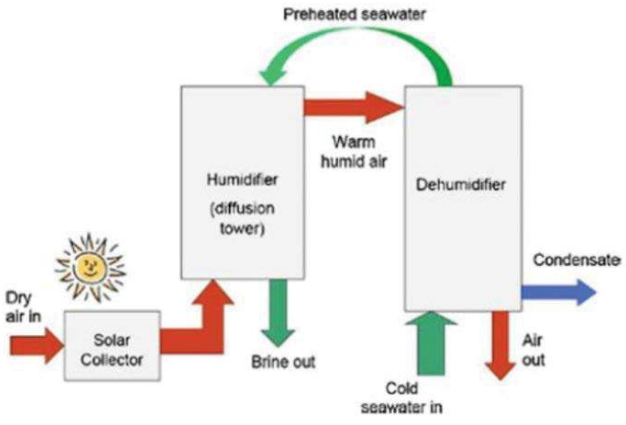

Fig. 1. The humidification–dehumidification cycle [2].

Maximum freshwater production reached 4,700 mL when the airflow rate was 200 kg/h. The freshwater yield increased with increasing mass flow rate of saline water (cooling water). The authors found that the freshwater rate increased with the decreasing temperature of the cooling water.

El-Shazly et al. [12] investigated which parameters most strongly influence the performance of a solar HDH unit with a packed bed of screens as a humidifier. The proposed HDH system included a humidifier, dehumidifier, and flat-plate solar collector for heating saline water. The packed-bed humidifier consisted of plastic screens with a bed length of 20–50 cm and a screen thickness of 1 mm. Hot saline water from the solar collector entered a sprayer at the top of the humidifier and air passed through the packing from the bottom of the humidifier for air humidification. The authors stated three objectives. The first objective was to investigate the performance of the HDH system using an external heating source for heating instead of a solar collector. The results indicated that freshwater productivity increased with increasing temperature of the inlet saline water temperature, increasing flow rate, and increasing thickness of the packing materials. The second objective was to define the most effective factors that influenced solar collector efficiency. The results showed that solar collector performance was enhanced when its angle was increased to as high as 45°. The third objective was to investigate HDH performance under different operating conditions. The results showed that HDH productivity increased as the inlet water flow rate was increased to 5 L/min and that the optimum packed column thickness was 40 cm; however, at higher flow rates and greater column thicknesses, productivity decreased. The authors also found that brine recycling to the solar collectors enhanced the HDH productivity of 214% compared with that in the absence of recycling.

Lawal et al. [8] conducted an investigated to enhance the performance of a HDH system operated by a heat pump. A mathematical model based on the first law of thermodynamics was developed to predict the efficiency of a closed-air–open-water (CAOW) water heating cycle and a modified air-heating cycle coupled with a heat pump. To enhance the GOR of the system, heat rejected from the condenser was used as a heat source in the humidifier. In addition, feed seawater was cooled via the cooling effect of the evaporator to increase the amount of condensed freshwater. The results showed that the optimum mass flow rate ratio was 0.63 and 1.3 with GORs of 8.88 and 7.63, respectively.

The effects of various parameters on the performance of HDH systems and evaluations of their performance using conventional energy analysis have been extensively reported [13–21]. However, differences between the types of energy and energy losses due to diminished energy quality have not been investigated. Exergy analysis is a potential tool for analyzing the performance of any thermal system. Exergetic (second-law) efficiency is the measure of the effective utilization of energy in the process and depends on both the systems and surroundings. The use of exergetic analysis can provide details about plant components that can be improved further. This analysis identifies the scope where the maximum energy losses occur and identify where improvement is needed [22]. Hou et al. [23] conducted exergy analysis of a solar multi-effect HDH

desalination process using pinch technology. The HDH system was composed of two main parts: (1) a wooden packed humidifier in which hot saline water was sprayed and contacted with air introduced by a fan and (2) a condenser (dehumidifier). As usual, seawater was fed to the dehumidifier for preheating and for recovering the latent heat of condensation; it was then further preheated in a flat-plate solar collector. Hot saline water was sprayed into the packed-bed humidifier for air humidification, and the air was cooled in the condenser by transferring the heat to the cold saline water, resulting in condensed freshwater. Exergy analysis was carried out on the solar multi-effect HDH desalination process (and could be applied to any thermal system) for design, optimization, and analysis of the system. The results indicated that exergy efficiencies of the HDH and the solar collector were low; thus, the HDH system requires further improvements to increase the exergy recovery rate. The solar collector exergy loss was 4.77%, and the dehumidifier exergy destruction was 5.7%.

To increase understanding of the improvement potential and optimization of HDH desalination systems, various research efforts have been focused on exergy and exergoeconomic analyses. Ghofrani and Moosavi [24] proposed and analyzed three advanced recycling HDHs using energy, exergy, exergoeconomic, and exergo-environmental assessments. One of the HDHs was heat-driven, and the other two were electrically driven systems. Zero liquid discharge to minimize the negative environmental impact of the desalination system was one of the advantages of this design. A new proposed brine recycling HDH desalination system coupled with a heat pump in which the humidifier was positioned before the evaporator was a novel feature of the study. The economic study results indicated that the cost of the proposed system (brine recycle (BR)–HDH–heat pump (HP)–evaporator after humidifier (EAH)) was lower than the costs of the other two systems. However, the BR–HDH–HP–EAH system has a lower environmental impact than the other two systems. Exergy analysis showed that the BR–HDH–HP (brine-recycle HDH system driven by heat) exhibits the highest second-law efficiency. The cooler, dehumidifier, and the heater were found to have the highest exergy destructions in the heat-driven system. By contrast, in the electricity-driven system, the compressor, expansion valve, and the dehumidifier were the highest exergy-destructive parts.

Kasaeian et al. [25] summarized most of the important studies involving productivity investigations, experimental works, mathematical modeling, and exergy and economic analyses of HDH systems. They made several recommendations for improving the performance and productivity of the systems, including calling for additional experimental studies of the actual behavior of HDH systems. Moreover, optimization of solar and hybrid desalination processes by considering various process conditions and variables is needed. Thus, the objective of the present work is to investigate the maximum productivity of a HDH system under actual experimental conditions. Accordingly, we present a theoretical investigation of the performance of a partial-recycle HDH cycle—specifically, a water-heated, CAOW cycle—with the objective of enhancing the condensation process and increasing the productivity of the system. Energy and exergy analyses of the solar heating system and HDH system were conducted to evaluate the performance and differentiate between these two analyses as well as to identify the components in which major exergy destructions occur.

2. System description

The proposed system, shown in Figs. 2 and 3, comprises two subsystems: (i) a solar collectors cycle and (ii) a HDH cycle. The solar collector cycle consists of six identical flat-plate solar collectors and a heat exchanger. The HDH desalination cycle consists of a humidifier (1 m × 0.6 m), dehumidifier (0.77 m × 0.54 m), pumps, blower, and an additional gas heater (5 L capacity, butane fuel).

2.1. Humidification–dehumidification desalination process

The HDH system investigated in the present work (Fig. 4) includes a partial-recycle water-heated, CAOW HDH cycle. This cycle differs from the conventional heated-water cycle because some of the preheated saline water that leaves the dehumidifier is recycled to the feed tank. In this way, the moisture in humid air is effectively condensed because of the maximum temperature difference between the hot humid air and the cold saline water. In addition, the portion of the saline water that completes the cycle is heated to a higher temperature than in a conventional cycle, leading to an effective humidification process. The preheated saline water then flows through the solar collectors to increase its temperature through indirect contact with the hot working fluid in the heat exchanger (water–ethylene glycol mixture). In the hybrid HDH system, saline water is further preheated using an additional gas heater. The heated saline water is sprinkled over a cellulosic packing material in the humidifier. The purpose of the packing material is to increase the contact surface area for effective mass and heat transfer. Some of the saline water evaporates in the air stream and the rest is discharged as brine from the humidifier bottom. Air is circulated by a blower from the bottom of the humidifier and through the packing materials, where it is heated and humidified as a result of direct contact with the sprayed hot saline water. The hot humid air leaves through the top of the humidifier to the top of the dehumidifier, where it is cooled on the outer surface of the shell and tube heat exchanger. The produced freshwater is then collected and measured.

2.2. Flat-plate solar collectors

The solar collector used in the experiments is a product of Inter Solar Egypt Company, Egypt. Six identical flat-plate solar collectors were used for heating the saline water (Fig. 5). The system comprises two cycles: the first is the closed cycle, where a mixture of water and ethylene glycol is heated in the six flat-plate solar collectors, and the second is an open cycle, where saline water is heated by indirect contact with the mixture in a heat exchanger made of 304 stainless steel. This innovative setup was designed to prevent corrosion of the collector materials by saline water.

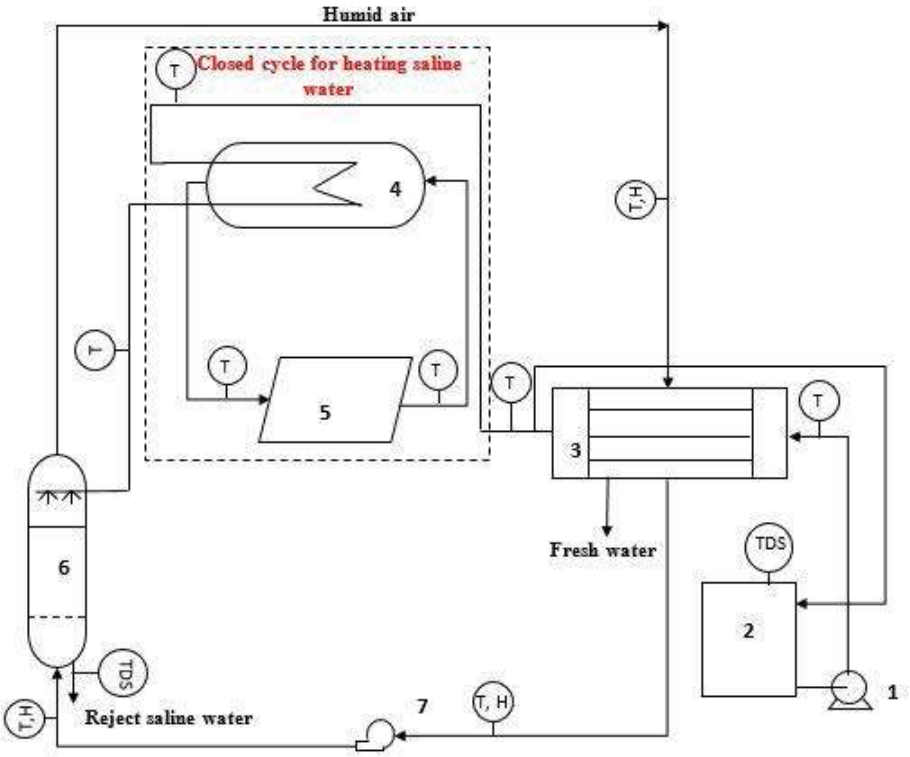

Fig. 2. Schematic of the partial-recycle solar HDH system: (1) feed pump; (2) saline water tank; (3) dehumidifier; (4) heat exchanger; (5) flat-plate solar collector; (6) humidifier; (7) blower.

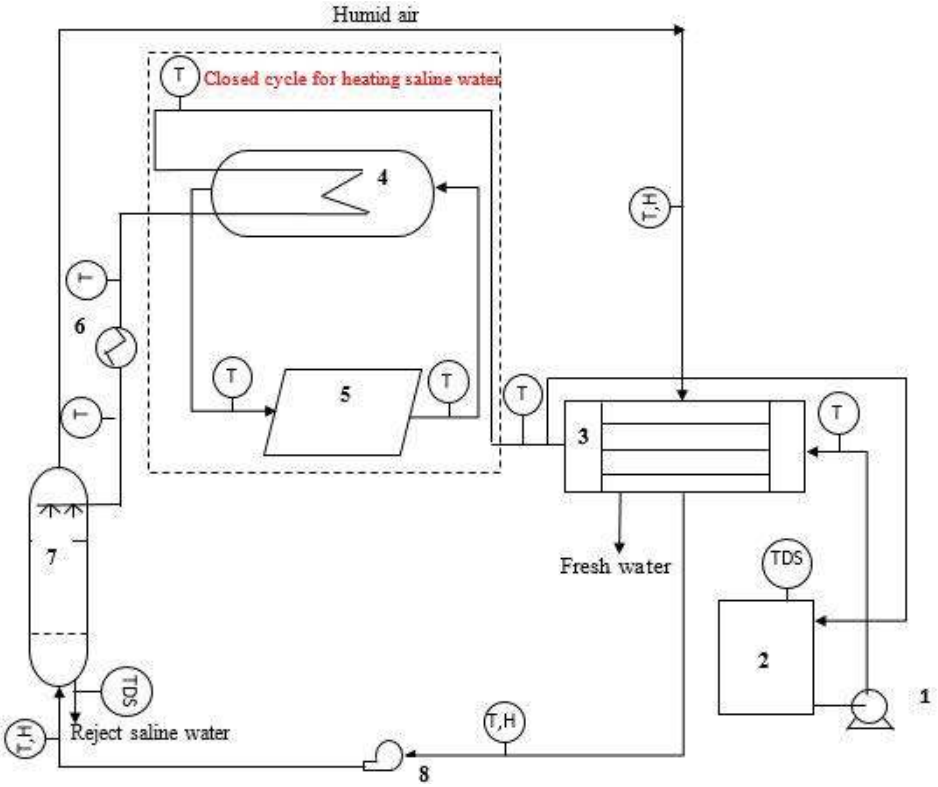

Fig. 3. Schematic of the partial-recycle hybrid HDH system: (1) feed pump; (2) saline water tank; (3) dehumidifier; (4) heat exchanger; (5) flat-plate solar collector; (6) additional gas heater; (7) humidifier; (8) blower.

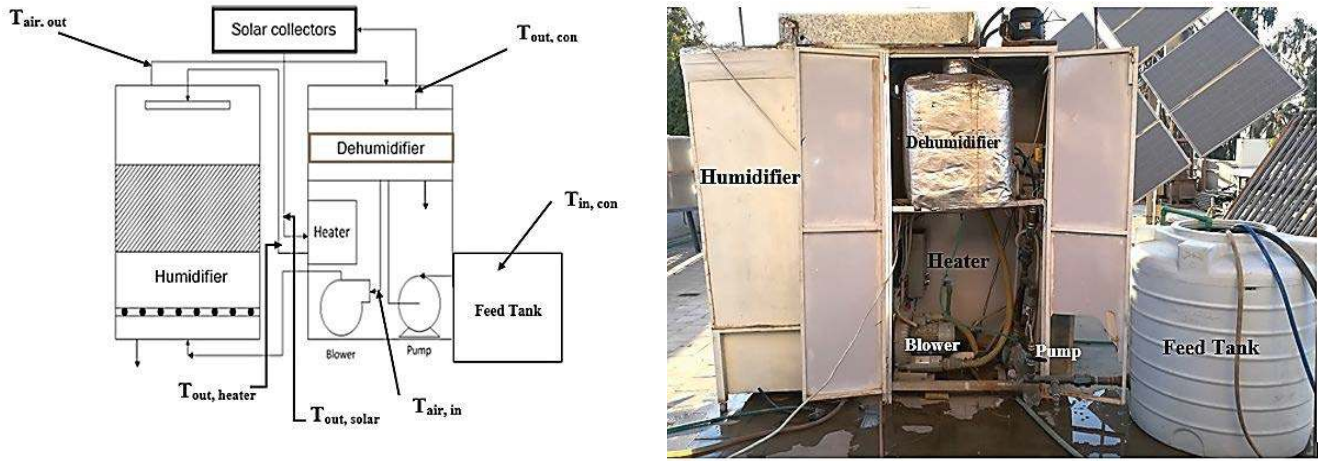

Fig. 4. Schematic and photograph of the experimental setup.

Fig. 5. Photographs of the flat-plate solar collectors.

3. Experimental work

To achieve the objectives of the current work, the performance of the proposed HDH system was investigated experimentally. Different experiments were designed to study the influence of various parameters on the performance of the solar collectors and on HDH productivity. The collector experiments were carried out on August 22, 23, and 24, 2017, in the Chemical Engineering Department of Minia University, Egypt (latitude 28.1194°N, longitude 30.7444°E). HDH experiments were performed during the period from May to September 2018 at the Faculty of Engineering, Minia University, Egypt. Inlet and outlet temperatures of the water in the flat-plate collectors and the heat exchanger were measured. The inlet and outlet temperatures of saline water in the humidifier and the dehumidifier were also measured. In addition, inlet and outlet temperatures and humidity of air in the humidifier and the dehumidifier were recorded. Figs. 4 and 5 show all of the positions at which different temperatures were measured. Temperature readings were recorded every 10 min for 7 h, resulting in 43 data points for 12 different measured temperatures. In each experiment, the productivity of the system was measured each hour during the experiment period. Solar energy was used as the energy source only in some of the experiments; the hybrid energy source was used in the others. Two different air blowers with different horsepower ratings (2 and 3 hp) and different flow rates were used to study the effect of airflow rates on productivity.

3.1. Uncertainty analysis

Uncertainty analysis is required to demonstrate the accuracy of experimental work. There are two types of uncertainty: type A and type B. Type A concerns random errors, whereas type B concerns systematic errors that can be evaluated on the basis of the specifications of the used measuring tools [26]. The uncertainty of the measured values expressed in the present work is exclusively type B. The measured parameters in the experiments include the inlet and outlet temperatures of air and water in the humidifier, dehumidifier, and solar collectors, the ambient temperature, and the solar intensity. *K*-type thermocouples with ±3°C accuracy were used for measuring temperatures.

A solar power meter (model SPM-1116SD) with an accuracy of ±10 W/m² was used to measure solar irradiance.

4. Mathematical model

We modeled the proposed HDH system presented in Fig. 4 under the following assumptions:

- The conditions are in a steady-state.
- Heat transfer to the surroundings can be neglected.
- Kinetic and potential energy changes can be neglected.
- No work transfer occurs between the system and the environment.
- The gas behaves as an ideal gas.

4.1. Solar system

4.1.1. Flat-plate solar collectors

4.1.1.1. Energy analysis

Under the assumption of steady-state conditions, the energy balance equation indicates that the useful energy output of the flat-plate solar collector is equal to the difference between the solar energy absorbed by the collector and thermal losses.

$$Q_g = A_c I_T \tag{1}$$

$$Q_l = A_c U_L \left(T_{\text{pm}} - T_a\right) \tag{2}$$

$$Q_u = Q_g - Q_l \tag{3}$$

$$Q_u = A_c \left(S - U_L \left(T_{\text{pm}} - T_a\right)\right) \tag{4}$$

where

$$-S = \left(\tau\alpha\right) I_T \tag{5}$$

Importantly, the heat-removal factor F_R is defined as the ratio between the actual useful energy gain if the whole collector surface is at the inlet fluid temperature and the useful energy gain:

$$F_R = \frac{\dot{m} C_p \left(T_{\text{fo}} - T_{\text{fi}}\right)}{A_c \left(S - U_L \left(T_{\text{fi}} - T_a\right)\right)} \tag{6}$$

Thus, the maximum possible useful energy equal to the actual energy gain:

$$Q_u = A_c F_R \left(S - U_L \left(T_{\text{fi}} - T_a\right)\right) \tag{7}$$

where U_L is the overall heat-loss coefficient, which is the sum of the top heat-loss coefficient U_t, bottom heat-loss coefficient U_b, and edge heat-loss coefficient U_e [28].

$$U_L = U_t + U_b + U_e \tag{8}$$

$$U_t = \left(\left(\left(\frac{N}{\frac{C}{T_{\text{pm}}}\left[\frac{\left(T_{\text{pm}} - T_a\right)}{\left(N + f\right)}\right]^e} + \frac{1}{h_w}\right)\right)^{-1}\right) + \frac{\sigma\left(T_{\text{pm}} + T_a\right)\left(T_{\text{pm}}^2 + T_a^2\right)}{\frac{1}{\varepsilon_p + 0.00591 N h_w} + \frac{2N + f - 1 + 0.133\varepsilon_p}{\varepsilon_g} - N} \tag{9}$$

$f = (1 + 0.089h_w - 0.1166h_w\varepsilon_p)(1 + 0.07866N)$

where $C = 520(1 - 0.000051B^2)$; $e = 0.430(1 - 100/T_{\text{pm}})$.

$$h_w = 5.7 + 3.8V_R \text{ [29]} \tag{10}$$

$$U_b = \frac{K}{L} \tag{11}$$

$$U_e = \frac{k_l A_e}{L_e A_p} \text{ [28]} \tag{12}$$

The first-law efficiency of the collector is defined as the ratio between the actual heat gain and the incident solar energy [30]:

$$\eta_I = \frac{Q_u}{I_T A_c} \tag{13}$$

4.1.1.2. Exergy analysis

Exergy is the maximum amount of useful work that can be obtained from a reversible process in which a given system reaches equilibrium with a defined environment [31]. Exergy can be classified into two types: thermomechanical and chemical exergy. The thermomechanical exergy can be defined as the maximum amount of work that can be obtained from the system when the temperature (T) and pressure (P) of the system differ from the temperature (T_o) and pressure (P_o) of the environment. The chemical exergy can be defined as the maximum theoretical work that can be obtained from the system when the concentration (W) of each component in the system differs from its concentration (W_o) in the environment at environment temperature and pressure [32].

The general exergy balance equation can be written in the following form [28]:

$$\text{Ex}_{\text{in}} - \text{Ex}_s - \text{Ex}_{\text{out}} - \text{Ex}_d = 0 \tag{14}$$

where Ex_{in} is the inlet exergy rate, Ex_s is the stored exergy rate, Ex_{out} is the outlet exergy rate, and Ex_d is the exergy loss rate.

Under steady-state conditions, stored exergy rate $\text{Ex}_s = 0$; thus, the exergy destruction equation can be expressed as:

$$\text{Ex}_d = \text{Ex}_{\text{in}} - \text{Ex}_{\text{out}} \tag{15}$$

The inlet exergy rate is the sum of the inlet exergy carried by the fluid and exergy radiation from the sun.

The inlet exergy rate carried by the fluid is expressed as:

$$\mathrm{Ex}_{\mathrm{in},f} = \dot{m}C_p\left(T_{\mathrm{fi}} - T_a - T_a\ln\left(\frac{T_{\mathrm{fi}}}{T_a}\right)\right) \tag{16}$$

Exergy radiation from the sun is expressed as:

$$\mathrm{Ex}_{\mathrm{in},Q} = I_T A_c\left(1-\frac{T_a}{T_s}\right) \tag{17}$$

The exergy rate outlet carried by the fluid flow is given as:

$$\mathrm{Ex}_{\mathrm{out},f} = \dot{m}C_p\left(T_{\mathrm{fo}} - T_a - T_a\ln\left(\frac{T_{\mathrm{fo}}}{T_a}\right)\right) \tag{18}$$

Exergy analysis enables the calculation of exergy losses due to heat loss from the absorber plate to the environment, exergy destruction due to temperature differences between the sun and absorber plate, exergy destruction due to radiation losses from the collector surface to the absorber plate, and exergy destruction due to the temperature difference between the fluid and absorber plate [28].

Exergy destruction rate due to heat loss from the absorber plate to the environment:

$$\mathrm{Ex}_{d,1} = U_L A_p\left(T_{\mathrm{pm}} - T_a\right)\left(1-\frac{T_a}{T_{\mathrm{pm}}}\right) \tag{19}$$

Exergy destruction rate due to the temperature difference between the sun and absorber plate:

$$\mathrm{Ex}_{d,2} = \left(\tau\alpha\right)I_T A_p T_a\left(\frac{1}{T_{\mathrm{pm}}}-\frac{1}{T_s}\right) \tag{20}$$

Exergy destruction rate due to radiation losses from the collector surface to the absorber plate:

$$\mathrm{Ex}_{d,3} = I_T\left[A_c - \left(\tau\alpha\right)A_p\right]\left(1-\frac{T_a}{T_s}\right) \tag{21}$$

Exergy destruction rate due to the temperature difference between the fluid and absorber plate:

$$\mathrm{Ex}_{d,4} = \dot{m}C_p T_a\left[\ln\left(\frac{T_{f,o}}{T_{f,i}}\right) - \frac{\left(T_{f,o}-T_{f,i}\right)}{T_{\mathrm{pm}}}\right] \tag{22}$$

The useful exergy rate can be calculated from the equation:

$$\mathrm{Ex}_u = \mathrm{Ex}_{\mathrm{out},f} - \mathrm{Ex}_{\mathrm{in},f} \tag{23}$$

The flat-plate solar collector efficiency is the ratio between the useful exergy rate and the solar radiation exergy rate (second-law efficiency) [27]:

$$\eta_{\mathrm{II}} = \frac{\mathrm{Ex}_{\mathrm{out},f} - \mathrm{Ex}_{\mathrm{in},f}}{I_T A_c\left(1-\frac{T_a}{T_s}\right)} \tag{24}$$

4.1.2. Shell and tube heat exchanger

4.1.2.1. Energy analysis

Useful energy absorbed by the fluid can be calculated from the following equation [33]:

$$Q_{u,h} = \dot{m}C_p\left(T_{f,o} - T_{f,i}\right) \tag{25}$$

First-law efficiency of the heat exchanger:

$$\eta_I = \frac{Q_{u,h}}{Q_u} \tag{26}$$

Overall energetic efficiency of the solar heating system:

$$\eta_I = \frac{Q_{u,h}}{I_T A_c} \tag{27}$$

4.1.2.2. Exergy analysis

Useful flow exergy delivered by saline water is determined using the following equation [34]:

$$\mathrm{Ex}_{u,h} = \dot{m}\left(\mathrm{Ex}_o - \mathrm{Ex}_i\right) \tag{28}$$

$$\mathrm{Ex}_{u,h} = \dot{m}\left(\left(H_{\mathrm{fo}} - H_{\mathrm{fi}}\right)\right) - T_o\left(S_{\mathrm{fo}} - S_{\mathrm{fi}}\right) \tag{29}$$

where

$$\left(H_{\mathrm{fo}} - H_{\mathrm{fi}}\right) = C_p\left(T_{\mathrm{fo}} - T_{\mathrm{fi}}\right) \tag{30}$$

$$\left(S_{\mathrm{fo}} - S_{\mathrm{fi}}\right) = C_p\ln\left(\frac{T}{T_o}\right) \text{ [35]} \tag{31}$$

Eq. (28) can be reduced to [36]:

$$\mathrm{Ex}_{u,h} = \dot{m}C_p\left(\left(T_{\mathrm{fo}} - T_{\mathrm{fi}}\right) - T_o\ln\left(\frac{T_{\mathrm{fo}}}{T_{\mathrm{fi}}}\right)\right) \tag{32}$$

Useful exergy can be calculated directly from the equation:

$$\mathrm{Ex}_{f,\mathrm{out}} - \mathrm{Ex}_{f,\mathrm{in}} = \dot{m}C_p\left(\left(T_{\mathrm{fo}} - T_{\mathrm{fi}}\right) - T_a\ln\left(\frac{T_{\mathrm{fo}}}{T_{\mathrm{fi}}}\right)\right) \tag{33}$$

Second-law efficiency of a heat exchanger can be given by the following equation:

$$\eta_{\mathrm{II}} = \frac{\mathrm{Ex}_{f,\mathrm{out}} - \mathrm{Ex}_{f,\mathrm{in}}}{\mathrm{Ex}_u} = \frac{\mathrm{Ex}_{u,h}}{\mathrm{Ex}_u} \tag{34}$$

Overall exergetic efficiency of the solar heating system:

$$\eta_{II} = \frac{Ex_{u,h}}{Ex_{Q,in}} \quad (35)$$

4.2. HDH system

4.2.1. Dehumidifier

4.2.1.1. Energy analysis

Mass balance:

The mass flow rate of produced freshwater is equal to the difference between the inlet and outlet humidity of air:

$$M_{fw} = M_a\left(d_{out} - d_{in}\right) \quad (36)$$

Energy balance:

$$M_{a2}h_{a2} + M_{w1in}h_{w1in} = M_{a1}h_{a1} + M_{w1out}h_{w1out} + M_{fw}h_{fw} \quad (37)$$

Effectiveness:

Effectiveness is defined as the ratio of the change in total enthalpy rate to the maximum possible change in total enthalpy rate [37,38]:

$$\varepsilon_{de} = \frac{h_{w,o} - h_{w,i}}{h_{w,o}^{ideal} - h_{w,i}} \quad (38)$$

4.2.1.2. Exergy analysis

Exergy destruction of the dehumidifier can be calculated as:

$$Ex_{d,d} = M_{a2}e_{a2} + M_{w1}\left(Ex_{w1in} - Ex_{w1out}\right) - M_{a1}Ex_{a1} - M_{fw}Ex_{fw} \text{ [39]} \quad (39)$$

Flow exergy of freshwater is calculated by:

$$Ex_{fw} = -R_v T_o \ln\left(\Phi_o\right) \text{ [40]} \quad (40)$$

Dehumidifier exergetic efficiency:

$$\eta_{II} = 1 - \frac{Ex_{d,d}}{\left(M_{a2}Ex_{a2} - M_{a1}Ex_{a1}\right)} \quad (41)$$

4.2.2. Humidifier

4.2.2.1. Energy analysis

Mass balance:

The inlet mass flow rate of air is equal to the outlet mass flow rate of air:

$$M_{a,in} = M_{a,out} \quad (42)$$

The inlet mass flow rate of water is equal to the outlet mass flow rate of water:

$$M_{w1} = M_{w2} + M_a\left(d_o - d_i\right) \quad (43)$$

Energy balance:

$$M_{w1}h_{w1} = M_{w2}h_{w2} + M_a\left(h_{ao} - h_{ai}\right) \quad (44)$$

Effectiveness:

$$\varepsilon_h = \frac{\dot{m}_{w,i}h_{w,i} - \dot{m}_{w,o}h_{w,o}}{\dot{m}_{w,i}h_{w,i} - \dot{m}_{w,o}h_{w,o}^{ideal}} \text{ [37]} \quad (45)$$

4.2.2.2. Exergy analysis

Exergy destruction of the humidifier can be written according to [39]:

$$Ex_{d,h} = M_{w1}e_{w1} + M_{a1}e_{a1} - M_{w2}e_{w2} - M_{a2}e_{a2} \quad (46)$$

Flow exergy of humid air at any point in the humidifier is calculated by:

$$Ex_n = \left[\left(C_p\right)_{da} + d_n\left(C_p\right)_v\right]\left(T_n - T_o\right) - T_o\left\{\left[\left(C_p\right)_{da} + d_n\left(C_p\right)_v\right]\ln\left(T_n/T_o\right) - \left(R_{da} + d_nR_v\right)\ln\left(P_n/P_o\right)\right\} + T_o\left[\begin{array}{l}\left(R_{da} + d_nR_v\right)\ln\left(\left(1+1.6078d_o\right)/\left(1+1.6078d_n\right)\right) + \\ 1.6078d_nR_{da}\ln\left(d_n/d_o\right)\end{array}\right] \text{[41]} \quad (47)$$

Humidifier exergetic efficiency:

$$\eta_{II} = \frac{Ex_{out}}{Ex_{in}} \quad (48)$$

$$Ex_d = Ex_{in} - Ex_{out} \quad (49)$$

$$\eta_{II} = 1 - \frac{E_d}{E_{in}} \quad (50)$$

$$\eta_{II} = 1 - \frac{Ex_d}{\left(M_{w1}e_{w1} - M_{w2}e_{w2}\right)} \quad (51)$$

5. Results and discussion

The behavior of the HDH system using both solar and hybrid energy sources was investigated experimentally and theoretically using conventional energy and exergy analyses. This section includes the experimental and analysis results for the flat-plate solar collectors and the HDH system. In these investigations, tests were carried out to determine the influence of the saline water flow rate on the outlet temperature of the water–ethylene glycol mixture from the collectors, the outlet temperature of saline water from the heat exchanger, and the energetic and exergetic efficiencies of the collectors. The effect of the saline water flow rate on the productivity of the solar and hybrid HDH systems and the effectiveness and exergetic efficiency of the humidifier is also investigated and discussed. The effect of the inlet air and saline water temperatures on exergy destruction in the

humidifier and the dehumidifier is investigated. The findings from the experimental study are presented graphically in Figs. 6–17. Table 1 gives an example of the experimental results obtained for various days in August 2017 and June/July 2018.

5.1. Flat-plate solar collectors

5.1.1. Effect of saline water flow rates on the outlet temperature in the solar collectors

Fig. 6 shows the variation of outlet water–ethylene glycol mixture temperature in the solar collectors as a function of time with three different saline water flow rates (0.03, 0.05, and 0.067 kg/s). The results show that the highest outlet water–ethylene glycol mixture temperature was 89°C at the lowest water flow rate (0.03 kg/s). Accordingly, the temperature of the mixture increased with decreasing saline water flow rate.

5.1.2. Effect of saline water flow rates on the outlet temperature in the heat exchanger

Fig. 7 shows the variation of the outlet saline water temperature as a function of time with three different saline water flow rates (0.03, 0.05, and 0.067 kg/s) in the heat exchanger. The highest recorded saline water outlet temperature was 74.5°C at 2:00 pm at 0.03 kg/s.

5.1.3. Effect of saline water flow rates on the energetic efficiency of the flat-plate solar collectors

The energetic efficiency of the solar collectors was calculated using traditional energy analysis, as expressed in Eqs. (1)–(13). However, traditional energy analysis is not a detailed or accurate tool for analyzing thermal systems because energetic efficiency of the solar collector is not a function of the inlet and outlet mixture temperatures. Fig. 8 shows the variation of the energetic efficiency of the solar collectors vs. time with different saline water flow rates. The energetic efficiency of the solar collector exhibits almost the same trend in the three experiments. The energy efficiencies range from 84.9% to 58.9%. However, a large difference is observed in the outlet mixture temperature between the experiment with the lowest flow rate (0.03 kg/s) and the two other experiments. This difference illustrates that conventional energy analysis is not a good tool to investigate the performance of any thermal system.

5.1.4. Effect of saline water flow rates on the exergetic efficiency of the flat-plate solar collectors

Energy analysis does not give a qualitative assessment of various losses that occur in system components. Thus, we used exergy analysis to provide both a quantitative and qualitative picture of various losses. Exergetic efficiency of the flat-plate solar collector was calculated using Eqs. (14)–(18), (23), and (24). The results indicate that the exergetic efficiency of the solar collectors was very small at both the beginning and end of the day because of the small difference between the inlet and outlet temperatures of the water–ethylene glycol mixture. The highest exergetic efficiency was 11.33% at 2:00 pm with the lowest flow rate (0.03 kg/s) and the highest outlet mixture temperature, as shown

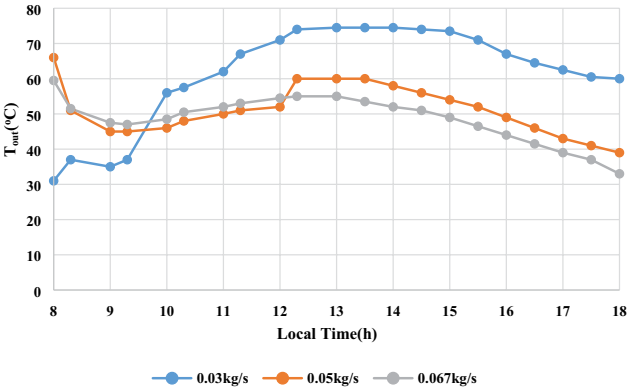

Fig. 7. Variation of outlet saline water temperature as a function of time at different flow rates in the heat exchanger (August 22–24, 2017, Minia University, Egypt).

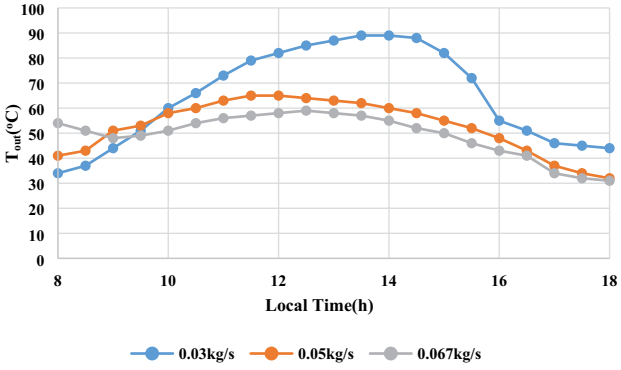

Fig. 6. Variation of outlet water–ethylene glycol mixture temperature in the solar collectors as a function of time at different flow rates of saline water (August 22–24, 2017, Minia University, Egypt).

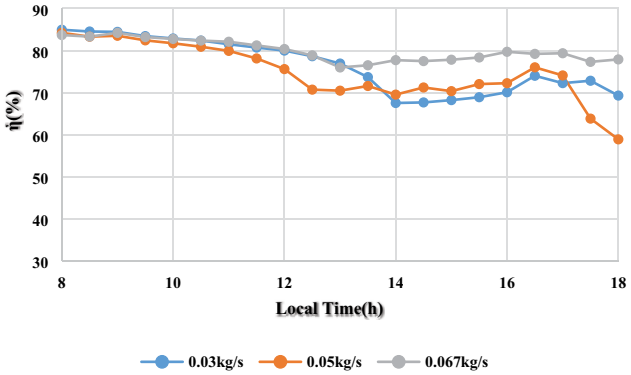

Fig. 8. Variation of the energetic efficiency of solar collectors vs. time at different flow rates (August 22–24, 2017, Minia University, Egypt).

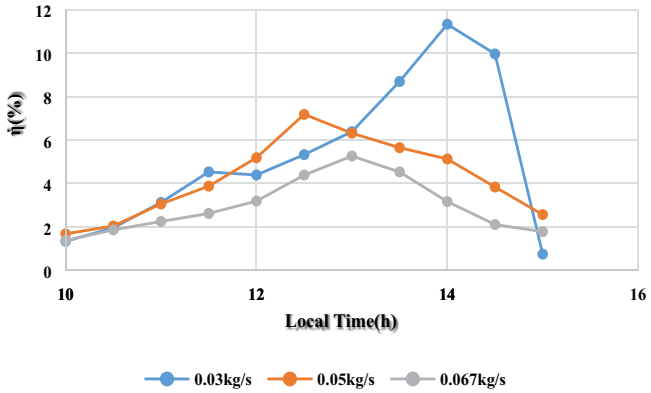

Fig. 9. Variation of the exergetic efficiency vs. time at different flow rates for the solar collector (August 22–24, 2017, Minia University, Egypt).

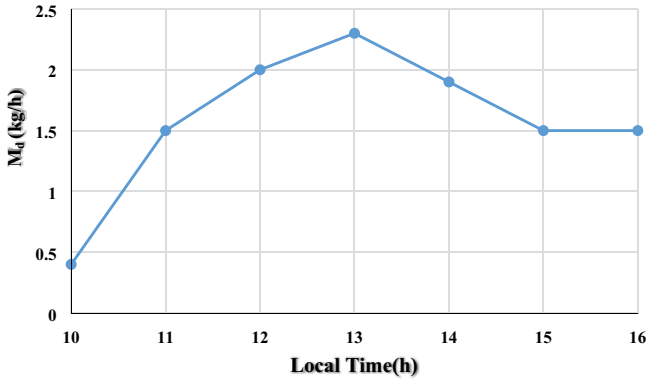

Fig. 10. Variation of freshwater production as a function of time during the day (June 21, 2018, Minia University, Egypt).

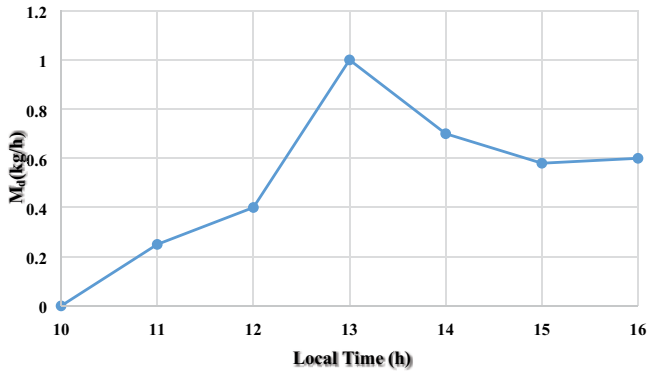

Fig. 11. Variation of freshwater production with time (June 24, 2018, Minia University, Egypt).

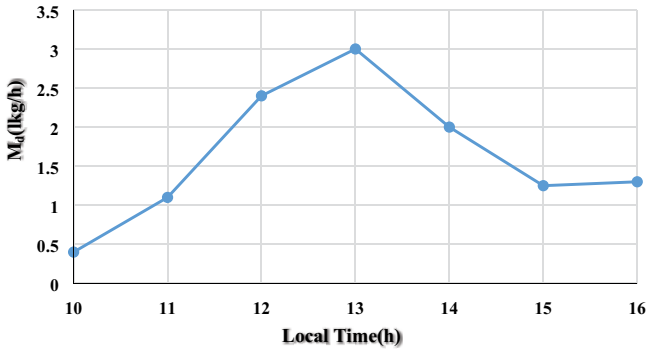

Fig. 12. Variation of freshwater production as a function of time (July 5, 2018, Minia University, Egypt).

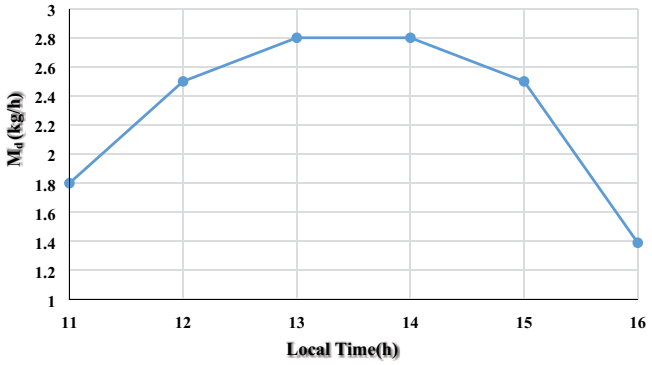

Fig. 13. Variation of freshwater production as a function of time (July 7, 2018, Minia University, Egypt).

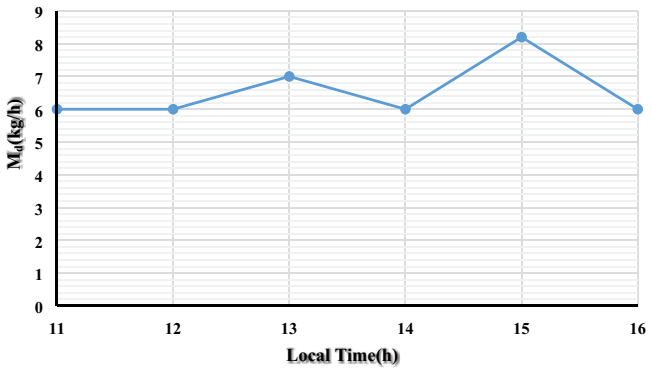

Fig. 14. Variation of freshwater production with time (May 7, 2018, Minia University, Egypt).

in Fig. 9. This result demonstrates that exergy analysis describes the actual performance of the system.

As the results show, the experiment with the lowest flow rate exhibits the highest outlet water–ethylene glycol mixture temperature, the highest exergetic efficiency, and the highest outlet saline water temperature. Thus, a comparison between exergetic and energetic efficiency of the solar heater system was carried out to describe the difference between them. The accumulated input and output energy were calculated using measured data and equations (saline water flow rate: 0.03 kg/s), as shown in Table 2.

Table 3 shows the accumulated input and output exergy for the solar heating system with a saline water flow rate of 0.03 kg/s.

Table 4 shows a comparison between energy and exergy analyses of the solar heating system. The heat exchanger has a low energetic efficiency; thus, the greatest energy losses occurred in it. However, the solar collectors exhibit the lowest

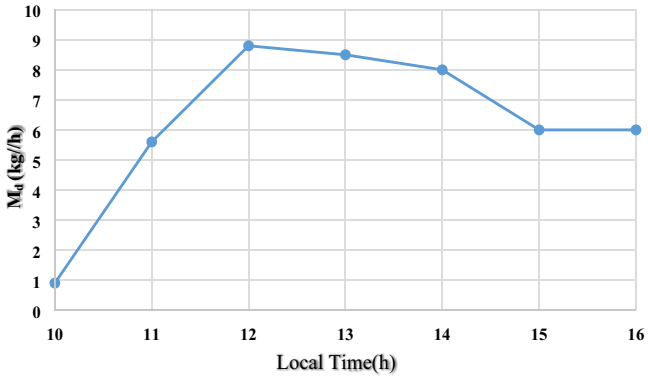

Fig. 15. Variation of freshwater production vs. time (June 20, 2018, Minia University, Egypt).

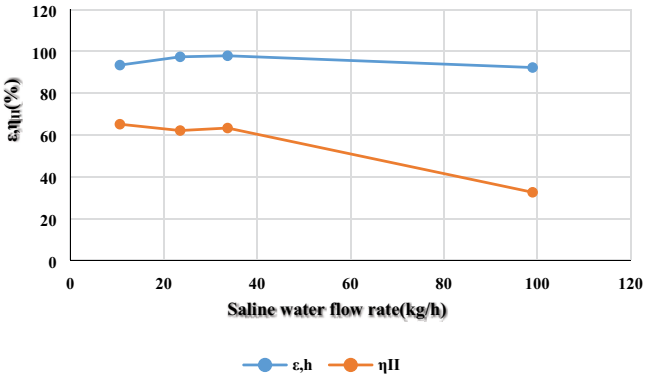

Fig. 16. Effect of saline water flow rate on humidifier effectiveness and exergetic efficiency.

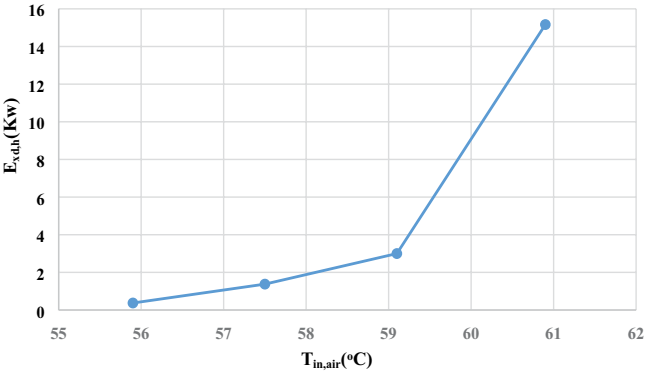

Fig. 17. Effect of inlet air temperature on the exergy destruction of the humidifier.

exergetic efficiency; the largest exergy destruction therefore occurred in the collectors.

The obtained results agree with those of Farzad et al. [42]. The exergetic efficiency of the flat-plate solar collector has been reported to be very low and to require substantial improvements because of the degradation of the exergy content of the solar energy from a high-quality 95% exergy content to a low exergy content of 10%–15% [34].

Energy analysis shows that the energetic efficiency of the system is very high at the lowest saline water flow rate. However, exergy analysis indicates a lower quality of this energy. This discrepancy is the difference between exergy and energy analyses. Energy analysis gives the quantity of energy irrespective of quality, whereas exergy analysis considers the quality of energy as well as its quantity.

Exergy analysis allows calculation of exergy destruction due to various causes, as discussed in section (4.1.1.2), using Eqs. (19)–(22). Exergy destruction in the solar collectors was calculated for the three saline water flow rates. Table 5 represents the calculated exergy destruction at 0.03 kg/s, and the two other experiments showed the same trend. The results show that the largest exergy destruction was E_{d2}.

5.2. HDH system

5.2.1. Solar HDH system

5.2.1.1. Effect of saline water flow rates on solar HDH system productivity using a 2 hp blower

Two experiments with different saline water flow rates using 2 hp blower (81 kg/h) were carried out to investigate the productivity of the HDH system under these conditions. Fig. 10 shows the variation of freshwater production as a function of time during the day. The highest product flow rate was 2.3 kg/h at 1:00 pm, and the average productivity was 1.6 kg/h on June 21 when the saline water flow rate was 33.67 kg/h.

Table 1
Results of some measured average values for various days

Date	I_T (W/m²)	M_w (kg/h)	$T_{in,solar}$ (°C)	$T_{out,solar}$ (°C)	$T_{in,he}$ (°C)	$T_{out,he}$ (°C)	$T_{in,deh}$ (°C)	T_a (°C)	$\Phi_{in,h}$ (%)	$\Phi_{out,h}$ (%)
22/08/2017	822.50	180	52.13	52.71	33.10	51.05	33.10	34.95	–	–
23/08/2017	776.88	108	64.35	64.71	33.80	61.14	33.80	37	–	–
24/08/2017	709.40	240	46.12	49.33	32.30	48.60	32.30	34.70	–	–
7/05/2018	843.60	23.50	62	77	33.23	62.62	32.87	28.46	23	100
20/06/2018	1,815	99.30	50.70	60	32.60	55.98	28.54	36.30	17.63	100
21/06/2018	1,748	33.60	62.53	76.7	33.11	64.30	30.29	37.36	15.32	100
24/06/2018	1,749	10.6	68.04	83.14	35.01	59.55	31.06	34.95	18.98	100
5/07/2018	–	12	76.87	75.2	36.73	75.32	31.96	35.84	19.58	100
7/07/2018	–	24.3	71.85	74.46	34.75	68.96	31.31	36.16	20.60	100

Table 2
Energy analysis of the solar heating system

System	Energy received (kW)	Energy delivered (kW)	Energy loss (kW)	Energy loss (%)	First-law efficiency (%)
Solar collector	215.59 ± 4.93	170.49 ± 4.19	45.09	20.92	79.08
Heat exchanger	170.49 ± 4.18	90.04 ± 5.63	80.46	47.19	52.81
Overall system	215.59 ± 4.93	90.03 ± 5.63	125.55	58.24	41.76

Table 3
Exergy analysis of the solar heating system

System	Exergy received (kW)	Exergy delivered (kW)	Exergy loss (kW)	Exergy loss (%)	Second-law efficiency (%)
Solar collector	196.68 ± 4.67	4.31 ± 0.45	192.38	97.81	2.19
Heat exchanger	4.21 ± 0.48	2.35 ± 0.15	1.859981	44.21	55.79
Overall system	196.69 ± 4.67	2.35 ± 0.15	194.34	98.81	1.19

Table 4
Comparison between first- and second-law analyses of the solar heating system

System	Energy loss (%)	Exergy loss (%)	First-law efficiency (%)	Second-law efficiency (%)
Solar collector	20.92	97.81	79.08	2.19
Heat exchanger	47.19	44.21	52.81	55.79
Overall system	58.24	98.81	41.76	1.19

Table 5
Exergy destruction in the solar collector due to various causes

Time (h)	E_{d1} (W)	E_{d2} (W)	E_{d3} (W)	E_{d4} (W)
9	19.49722	14,946.03	3,691.87	0.089257
9.5	44.43138	13,380.38	3,426.768	0.137547
10	54.66677	12,204.43	3,159.581	0.159654
10.5	63.67916	11,326.67	2,958.815	0.177522
11	84.14934	10,364.85	2,759.614	0.199412
11.5	99.83743	9,530.835	2,570.842	0.206493
12	109.9032	8,762.297	2,382.071	0.153798
12.5	118.757	7,419.382	2,030.288	0.135942
13	123.7153	6,111.995	1,678.505	0.117255
13.5	123.2987	4,503.873	1,236.507	0.08916
14	115.0979	2,911.22	794.5102	0.052778
14.5	107.1506	2,839.118	770.2098	0.03597
15	95.3384	2,775.33	745.9093	0.003605

The productivity of the HDH system powered by solar energy was measured at a low saline feedwater flow rate of 10.58 kg/h. Fig. 11 shows the variation of freshwater production vs. time. This figure shows that the productivity decreased by decreasing the saline water flow rate.

5.2.1.2. Effect of saline water flow rates on solar HDH system productivity (3 hp)

The performance and productivity of the HDH system powered by solar energy were measured at a high air flow rate using a 3 hp blower with a flow rate of 98 kg/h. Fig. 12 shows the variation of freshwater production as a function of time at a saline water flow rate of 12 kg/h on July 5. The maximum productivity was 3 kg/h at 1:00 pm, and the average production rate was found to be 1.6 kg/h.

Fig. 13 shows the variation of freshwater production as a function of time with a saline water flow rate of 24 kg/h on July 7. The maximum productivity was 2.8 kg/h at 1:00 pm, and the average production rate was 2.3 kg/h. The results show that freshwater productivity increased with increasing air and saline water flow rates.

Table 6
Productivity comparison of the proposed system with other HDH desalination systems

Systems	Productivity (kg/h)	References
HDH operated by heat pump	8.5	Lawal et al. [3]
HDH operated by heat pump	11.99	Lawal et al. [4]
HDH with electrical water heaters	8.22	El-Agouz et al. [43]
HDH system with modified air heater	0.82	Muthusamy et al. [44]
Multi-stage solar HDH	3.4	Wu et al. [5]
Solar HDH	15.23 kg/m^2 d	Rajaseenivasan et al. [6]
HDH with mass extraction	144 L/d	Lawal et al. [9]
(CAOW) partial-recycle hybrid HDH system	8.8	Present study
(CAOW) partial-recycle solar HDH system	3	Present study

5.2.2. Hybrid HDH system

5.2.2.1. Effect of saline water flow rates on hybrid HDH system productivity

Experiments were performed with hybrid energy using an additional heater to enhance the humidification process. Fig. 14 shows the variation of freshwater production as a function of time on May 7 with a 23.5 kg/h saline water flow rate. The maximum productivity was 8.2 kg/h at 3:00 pm, and the average production rate was 6.5 kg/h.

The productivity of HDH system was investigated at the maximum saline water flow rate of 99 kg/h. Fig. 15 presents the variation of freshwater production with time on May 7. The maximum productivity was 8.8 kg/h at 12:00 pm, and the average production rate was 7.2 kg/h.

5.2.2.2. Effect of saline water flow rates on the effectiveness and exergetic efficiency of the humidifier

Fig. 16 shows the effect of saline water flow rates on the effectiveness and exergetic efficiency of the humidifier. The effectiveness was almost constant as the saline water flow rate was varied; however, the exergetic efficiency increased with decreasing saline water flow rate.

5.2.2.3. Effect of inlet air temperature on the exergy destruction of the humidifier

Fig. 17 shows the effect of the inlet air temperature on the exergy destruction of the humidifier. Exergy destruction of the humidifier decreases with decreasing inlet air temperature.

5.3. Productivity comparison of the proposed HDH system with other HDH desalination systems

The productivity comparison of the currently proposed system with other HDH desalination systems is presented in Table 6. It can be concluded that the current proposed CAOW partial recycle HDH desalination system is competitive with HDH desalination systems in terms of productivity.

6. Conclusion

An experimental investigation of a partial-recycle solar/hybrid HDH system at different saline water and air flow rates and different temperatures was presented. A performance evaluation of the solar heating system and HDH system using energy and exergy analyses was performed. Exergy destruction in the solar collectors and HDH cycles was calculated. The following are the major conclusions of the present study:

- Second-law (exergetic) efficiency of the solar heater was very low (2.19%) because of the high exergy destruction of the solar energy.
- Exergy analysis showed that the largest exergy destruction occurred in the solar collectors.
- The largest contributor to exergy destruction in the solar collectors was the difference between the plate and sun temperatures, which can be decreased by increasing the inlet saline water temperature via an efficient recycling system.
- For the HDH system, the highest destruction rate occurred in the dehumidifier.
- The exergy destruction rate in the humidifier increased at high saline water flow rates.
- For the HDH system powered by solar energy only, the highest productivity was 3 kg/h; for the HDH system powered by the hybrid solar traditional energy, the highest productivity was 8.8 kg/h.
- Exergetic destruction in the dehumidifier can be reduced by increasing the inlet saline water temperature.
- Exergy destruction in the humidifier can be decreased by lowering the inlet air temperature.

Acknowledgment

The Misr El Kheir Foundation is gratefully acknowledged for the support of this work under scientific grant agreement between Misr El Kheir foundation and Minia University-Faculty of Engineering.

Symbols

I_T — Solar intensity, W/m^2
M_w — Saline water flowrate, kg/h

η_I — Energetic efficiency
η_{II} — Exergetic efficiency
A_c — Area of collector, m^2
B — Tilt angle
C_p — Specific heat at constant pressure, kJ/kg K
$(C_p)_{da}$ — Specific heat capacity of vapor, kJ/kg K
$(C_p)_v$ — Specific heat capacity of vapor, kJ/kg K
C_v — Specific heat at constant volume, kJ/kg K
D — Humidity ratio of air, kg_{wv}/kg_{da}
d_o — Humidity ratio at dead state, kg_{wv}/kg_{da}
E — Energy of the system, kJ
Ex — Total exergy, kJ
Ex — Specific exergy, kJ/kg
ε_g — Emissivity of glass
ε_p — Emissivity of absorber plate
F_R — Heat removal factor
G — Acceleration of gravity, m/s^2
H — Specific enthalpy, kJ/kg
h_w — Wind heat transfer coefficient, W/m^2 K
K — Thermal conductivity of insulation, W/m K
L — Thickness of insulation, m
N — Number of glass covers
P — Pressure, kpa
Q — Amount of heat, kJ
R — Universal gas constant, kJ/kg_{mol} K
R_{da} — Gas constant of dry air, kJ/kg K
R_v — Gas constant of vapor, kJ/kg K
S — Entropy, kJ/kg K
$T_{in,solar}$ — Inlet temperature of water-ethylene glycol in the solar collector, °C
$T_{out,solar}$ — Outlet temperature of water-ethylene glycol in the solar collector, °C
$T_{in,he}$ — Inlet temperature of saline water in the heat exchanger in the solar system, °C
$T_{out,he}$ — Outlet temperature of saline water in the heat exchanger in the solar system, °C
$T_{in,deh}$ — Inlet temperature of saline water in the dehumidifier, °C
$T_{out,deh}$ — Outlet temperature of saline water in the dehumidifier, °C
$T_{air,in}$ — Inlet air temperature, °C
T_a — Ambient temperature, °C
T_s — Sun temperature, °C
U — Internal energy of the system, kJ
U_b — Bottom heat loss coefficient, W/m^2 K
U_e — Edge heat loss coefficient, W/m^2 K
U_L — Overall heat transfer coefficient, W/m^2 K
U_t — Top heat loss coefficient, W/m^2 K
V — Specific volume, m^3/kg
V — Velocity, m/s
V_R — Wind velocity, m/s
W — Amount of heat, kJ
Z — Height of the system, m
E — Effectiveness
Φ — Relative humidity percentage of air
Φ_o — Relative humidity percentage of air at dead state
$\Phi_{in,h}$ — Relative humidity of inlet air in the humidifier
$\Phi_{out,h}$ — Relative humidity of outlet air in the humidifier
α — Absorptance
σ — Stefan Boltzmann constant, W/m^2 K^4
τ — Transmittance

Subscripts

c — Combined system
o — Dead state
s — System
e — Environment
gen — Generation
cv — Control volume
out — Outlet
in — Inlet
mix — Water-Ethylene glycol mixture
d — Destruction
g — Gain
pm — Mean plate
a — Ambient
u — Useful
fw — Freshwater

References

[1] W. Abdelmoez, E.A. Ashour, N.M. Sayed, Water desalination by humidification–dehumidification technology with performance evaluation using exergy analysis, Desal. Water Treat., 148 (2019) 1–19.
[2] W. Abdelmoez, M.S. Mahmoud, T.E. Farrag, Water desalination using humidification–dehumidification (HDH) technique powered by solar energy: a detailed review, Desal. Water Treat., 52 (2014) 4622–4640.
[3] D.U. Lawal, M.A. Antar, A. Khalifa, S.M. Zubair, Heat pump operated humidification–dehumidification desalination system with option of energy recovery, Sep. Sci. Technol., (2020) 1–20, https://doi.org/10.1080/01496395.2019.1706576.
[4] D.U. Lawal, M.A. Antar, A. Khalifa, S.M. Zubair, F. Al-Sulaiman, Experimental investigation of heat pump driven humidification–dehumidification desalination system for water desalination and space conditioning, Desalination, 475 (2020) 114–199.
[5] G. Wu, H.F. Zheng, X.L. Ma, C. Kutlu, Y.H. Su, Experimental investigation of a multi-stage humidification–dehumidification desalination system heated directly by a cylindrical Fresnel lens solar concentrator, Energy Convers. Manage., 143 (2017) 241–251.
[6] T. Rajaseenivasan, K. Srithar, Potential of a dual purpose solar collector on humidification–dehumidification desalination system, Desalination, 404 (2017) 35–40.
[7] S.M. Zubair, M.A. Antar, S.M. Elmutasim, D.U. Lawal, Performance evaluation of humidification–dehumidification (HDH) desalination systems with and without heat recovery options: an experimental and theoretical investigation, Desalination, 436 (2018) 161–175.
[8] D. Lawal, M. Antar, A. Khalifa, S. Zubair, F. Al-Sulaiman, Humidification–dehumidification desalination system operated by a heat pump, Energy Convers. Manage., 161 (2018) 128–140.
[9] D.U. Lawal, M.A. Antar, A. Aburub, M. Aliyu, Performance assessment of a cross-flow packed-bed humidification–dehumidification (HDH) desalination system – the effect of mass extraction, Desal. Water Treat., 104 (2018) 28–37.
[10] L. Xu, Y.-P. Chen, P.-H. Wu, B.-J. Huang, Humidification–dehumidification (HDH) desalination system with air-cooling condenser and cellulose evaporative pad, Water, 142 (2020) 1–14, https://doi.org/10.3390/w12010142.
[11] P.H. Gao, L.X. Zhang, H.F. Zhang, Performance analysis of a new type desalination unit of heat pump with humidification–dehumidification, Desalination, 220 (2008) 531–537.

[12] A.H. El-Shazly, M.M. El-Gohary, M.E. Ossman, Performance characteristics of a solar humidification–dehumidification unit using packed bed of screens as the humidifier, Desal. Water Treat.,16 (2010) 17–28.
[13] S. Farsad, A. Behzadmehr, Analysis of a solar desalination unit with humidification–dehumidification cycle using DoE method, Desalination, 278 (2011) 70–76.
[14] T. Rajaseenivasan, K. Srithar, An investigation into a laboratory scale bubble column humidification–dehumidification desalination system powered by biomass energy, Energy Convers. Manage., 139 (2017) 232–244.
[15] F.A. Al-Sulaiman, M.I. Zubair, M. Atif, P. Gandhidasan, S.A. Al-Dini, M.A. Antar, Humidification–dehumidification desalination system using parabolic trough solar air collector, Appl. Therm. Eng., 75 (2015) 809–816.
[16] K.M. Chehayeb, G.P. Narayan, S.M. Zubair, J.H. Lienhard V, Thermodynamic balancing of a fixed-size two-stage humidification–dehumidification desalination system, Desalination, 369 (2015) 125–139.
[17] K.M. Chehayeb, G.P. Narayan, S.M. Zubair, J.H. Lienhard V, Use of multiple extractions and injections to thermodynamically balance the humidification–dehumidification desalination system, Int. J. Heat Mass Transfer, 68 (2014) 422–434.
[18] A.M.I. Mohamed, N.A. El-Minshawy, Theoretical investigation of solar humidification–dehumidification desalination system using parabolic trough concentrators, Energy Convers. Manage., 52 (2011) 3112–3119.
[19] J.-J. Hermosillo, C.A. Arancibia-Bulnes, C.A. Estrada, Water desalination by air humidification: mathematical model and experimental study, Sol. Energy, 86 (2012) 1070–1076.
[20] M. Al-Sahali, H.M. Ettouney, Humidification–dehumidification desalination process: design and performance evaluation, Chem. Eng. J., 143 (2008) 257–264.
[21] K.H. Mistry, A. Mitsos, J.H. Lienhard V, Optimal operating conditions and configurations for humidification–dehumidification desalination cycles, Int. J. Therm. Sci., 50 (2011) 779–789.
[22] C. Muthusamy,K. Srithar, Energy and exergy analysis for a humidification–dehumidification desalination system integrated with multiple inserts, Desalination, 367 (2015) 49–59.
[23] S.B. Hou, D.Q. Zeng, S.Q. Ye, H.F. Zhang, Exergy analysis of the solar multi-effect humidification–dehumidification desalination process, Desalination, 203 (2007) 403–409.
[24] I. Ghofrani, A. Moosavi, Energy, exergy, exergoeconomics, and exergoenvironmental assessment of three brine recycle humidification–dehumidification desalination systems applicable for industrial wastewater treatment, Energy Convers. Manage, 205 (2020) 112349.
[25] A. Kasaeian, S. Babaei, M. Jahanpanah, H. Sarrafha, A.S. Alsagri, S. Ghaffarian, W.-M. Yan, Solar humidification–dehumidification desalination systems: a critical review, Energy Convers. Manage, 201 (2019) 112–129.
[26] J.A. Esfahani, N. Rahbar, M. Lavvaf, Utilization of thermoelectric cooling in a portable active solar still — an experimental study on winter days, Desalination, 269 (2011) 198–205.
[27] S. Farahat, F. Sarhaddi, H. Ajam, Exergetic optimization of flat plate solar collectors, Renewable Energy, 34 (2009) 1169–1174.
[28] Z. Ge, H.T. Wang, H. Wang, S.Y. Zhang, X. Guan, Exergy analysis of flat plate solar collectors, Entropy, 16 (2014) 2549–2567.
[29] A. Ucar, M. Inallı, Thermal and exergy analysis of solar air collectors with passive augmentation techniques, Int. Commun. Heat Mass Transfer, 33 (2006) 1281–1290.
[30] J.A. Duffie, W.A. Beckman, Solar Engineering of Thermal Processes, 4th ed., John Wiley & Sons, United States of America, 2013.
[31] F. Signorato, M. Morciano, L. Bergamasco, M. Fasano, P. Asinari, Exergy analysis of solar desalination systems based on passive multi-effect membrane distillation, Energy Rep., 6 (2020) 445–454.
[32] M.H. Sharqawy, J.H. Lienhard V, S.M. Zubair, On exergy calculations of seawater with applications in desalination systems, Int. J. Therm. Sci., 50 (2011) 187–196.
[33] H. Esen, M. Inalli, M. Esen, K. Pihtili, Energy and exergy analysis of a ground-coupled heat pump system with two horizontal ground heat exchangers, Build Environ., 42 (2007) 3606–3615.
[34] N. Singh, S.C. Kaushik, R.D. Misra, Exergetic analysis of a solar thermal power system, Renewable Energy, 19 (2000) 135–143.
[35] Y.A. Cengel, M.A. Boles, Thermodynamics: An Engineering Approach, 5th ed., McGraw-Hill, Penn Plaza, New York, USA, 2006, pp. 357–377.
[36] K. Gnana Sundari, V. Ponnaganti, T.M.N. Kumar, Exergy analysis of a low temperature thermal desalination system, Int. J. Mech. Eng. Robot. Res., 2 (2013) 284–289.
[37] G.P. Narayan, K.H. Mistry, M.H. Sharqawy, S.M. Zubair, J.H. Lienhard V, Energy effectiveness of simultaneous heat and mass exchange devices, Front. Heat Masss Transfer, (2010) 1–39, doi: 10.5098/hmt.v1.2.3001.
[38] G.P. Narayan, J.H. Lienhard V, S.M. Zubair, Entropy generation minimization of combined heat and mass transfer devices, Int. J. Therm. Sci., 49 (2010) 2057–2066.
[39] M.A. Elhaj, J.S. Yassin, Exergy analysis of a solar humidification–dehumidification desalination unit, Int. J. Mech. Ind. Sci. Eng., 7 (2013) 622–626.
[40] A. Bejan, Advanced Engineering Thermodynamics,1st ed., John Wiley & Sons, Inc., Singapore, 1988.
[41] I. Dincer, A.Z. Sahin, A new model for thermodynamic analysis of a drying process, Int. J. Heat Mass Transfer, 47 (2004) 645–652.
[42] F. Jafarkazemi, E. Ahmadifard, Energetic and exergetic evaluation of flat plate solar collectors, Renewable Energy, 56 (2013) 55–63.
[43] S.A. El-Agouz, A new process of desalination by air passing through seawater based on humidification–dehumidification process, Energy, 35 (2010) 5108–5114.
[44] C. Muthusamy, M. Gowtham, S. Manickam, M. Manjunathan, K. Srithar, Enhancement of productivity of humidification–dehumidification desalination using modified air heater, Desal. Water Treat., 56 (2015) 3294–3304.